Selective oxidation of cyclohexene through gold functionalized silica monolith microreactors

Mohammed T. Alotaibi [a], Martin J. Taylor [abc], Dan Liu [a], Simon K. Beaumont [d] and Georgios Kyriakou [abc]*

[a] Department of Chemistry, The University of Hull, Cottingham Rd, Hull HU6 7RX, United Kingdom

[b] European Bioenergy Research Institute, Aston University, Aston Triangle, Birmingham, B4 7ET, United Kingdom

[c] Chemical Engineering and Applied Chemistry, Aston University, Aston Triangle, Birmingham B4 7ET, United Kingdom

[d] Department of Chemistry, Durham University, South Road, Durham DH1 3LE, United Kingdom

*Corresponding Author Email: g.kyriakou@aston.ac.uk

Keywords: Monolith, Selective oxidation, Cyclohexene, Epoxidation, Gold

Abstract

Two simple, reproducible methods of preparing evenly distributed Au nanoparticle containing mesoporous silica monoliths are investigated. These Au nanoparticle containing monoliths are subsequently investigated as flow reactors for the selective oxidation of cyclohexene. In the first strategy, the silica monolith was directly impregnated with Au nanoparticles during the formation of the monolith. The second approach was to pre-functionalize the monolith with thiol groups tethered within the silica mesostructure. These can act as evenly distributed anchors for the Au nanoparticles to be incorporated by flowing a Au nanoparticle solution through the thiol functionalized monolith. Both methods led to successfully achieving even distribution of Au nanoparticles along the length of the monolith as demonstrated by ICP-OES. However, the impregnation method led to strong agglomeration of the Au nanoparticles during subsequent heating steps while the thiol anchoring procedure maintained the nanoparticles in the range of 6.8 ± 1.4 nm. Both Au nanoparticle containing monoliths as well as samples with no Au incorporated were tested for the selective oxidation of cyclohexene under constant flow at 30 °C. The Au free materials

were found to be catalytically inactive with Au being the minimum necessary requirement for the reaction to proceed. The impregnated Au-containing monolith was found to be less active than the thiol functionalized Au-containing material, attributable to the low metal surface area of the Au nanoparticles. The reaction on the thiol functionalized Au-containing monolith was found to depend strongly on the type of oxidant used: tert-butyl hydroperoxide (TBHP) was more active than H_2O_2, likely due to the thiol induced hydrophobicity in the monolith.

1. Introduction

The catalytic properties and surface chemistry of Au has been the focus of intense research over the past two decades.[1,2] Gold nanoparticles have been identified as catalytically active for a number of diverse reactions including low temperature CO oxidation [3], selective oxidation reactions [4], hydrogen peroxide formation from O_2 and H_2 [5], coupling reactions [6,7] and hydrogenations.[8] Selective oxidation reactions are of prime economic importance in a diverse range of applications from the production of fine chemicals and synthetic fibers to polymers and paints.

Continuous-flow catalytic microreactors have long been envisaged as a practical, economic, environmentally friendly method of carrying out reactions of importance for a variety of industries including fine chemicals.[9,10] Microreactors present many key advantages over the traditionally used batch reactors.[9] Such advantages include continuous flow operation, ease of separation of the catalyst from reactants and products and the ease of sampling without contamination when removing an aliquot. Of particular importance is the ability to obtain accurate and reproducible control over the reaction conditions such as temperature, pressure and reaction solvent.[9,11] Furthermore, monolithic devices (microreactors containing a porous network of typically silica or other oxide materials) can be functionalized extensively with enzymes[12], magnetic nanoparticles[11] and other functional groups[12–14] in order to tailor their catalytic properties such as selectivity and activity. [10,15]. The incorporation of metal nanoparticles in monolithic structures in particular has received attention for its applications in, chromatography [15,16], metal adsorption for contaminant purification [17], C-C coupling reactions [18], reduction of nitrophenols [19] and CO oxidation reactions. [20] In the case of oxidation it has been reported that silica monoliths loaded with either Pt or Pd nanoparticles presented conversions 2.5x higher in microreactors than when using powder catalysts. This shows that using microreactor technology for catalytic oxidation reactions enhances the catalytic ability of precious metal catalysts.[20] A

major challenge in all cases however is to evenly functionalize the catalytically active species along the length of the monolithic microreactor, which is key to maximizing efficient reaction control.

Here we have used a simple reproducible method to synthesize mesoporous silica monolithic reactors and investigated two strategies for evenly functionalizing them with gold nanoparticles along their length. In this way we are aiming to combine (i) a continuous flow monolithic system, which offers a variety of operational and economic benefits with (ii) the unique catalytic properties of Au in selective oxidation catalysis. Two different methods were used to achieve even Au nanoparticle distribution within the monoliths. Firstly, simple impregnation of Au nanoparticles into the monolith during the monolith's formation ensures even / random positioning of the nanoparticles as a result of solution phase mixing. Secondly, tethering thiol groups into the mesoporous structure of the monolith using 3-mercaptopropyl)trimethoxysilane allows the sulfur groups to act as anchors for the Au nanoparticles which can then be passed through the monolith and be tethered to the thiol groups. As the small thiol groups can diffuse readily through the monolith and react with surface hydroxyls to produce an even coverage this allows Au nanoparticles to be flowed through the reactor until some saturation coverage of the thiols is reached, at which point the even distribution of the thiol groups confers a similarly even distribution within the monolith upon the anchored gold nanoparticles. As will be shown, both methods do succeed in distributing the gold evenly along the length of the reactor. However, in the case of the impregnated method heat treatment during synthesis, results to heavily agglomerated Au nanoparticles. In contrast, the material containing thiol groups that can act as anchoring sites for the Au nanoparticles led to a material that was not only evenly dispersed along the length of the monolith but also exhibits a smaller particle size and more uniform particle size distribution.

The materials synthesized were tested for the selective oxidation of cyclohexene. [21] The reason behind the choice of cyclohexene as the test molecule is the volume of data that exists in the literature, which allows for the appropriate choice of reaction conditions.[22] The oxidation of cyclohexene has been utilised as a model reaction in selective oxidation studies.[23–25] Two common liquid phase oxidants were employed: hydrogen peroxide (H_2O_2) and tert-butyl hydroperoxide (TBHP). [22,26,27] The Au free monoliths were found to be catalytically inert at 30 $^{\circ}$C. The presence of Au was the minimum necessary requirement

for the selective oxidation reaction to proceed. Both Au functionalized monoliths were found to be active for the selective oxidation of cyclohexene (Fig. 1) with the thiol functionalized monolith being more active as compared to the impregnated monolith due to the better dispersity and higher surface area of Au. The oxidation reaction on the Au-thiol functionalized monolith was found to depend on the type of oxidant used with TBHP being more active than H_2O_2. We suggest this can be attributed to the thiol modifier (containing propyl groups) rendering the silica surface of the monolith more hydrophobic than the hydroxyl termination of the bare silica surface and so favouring the organic oxidant.

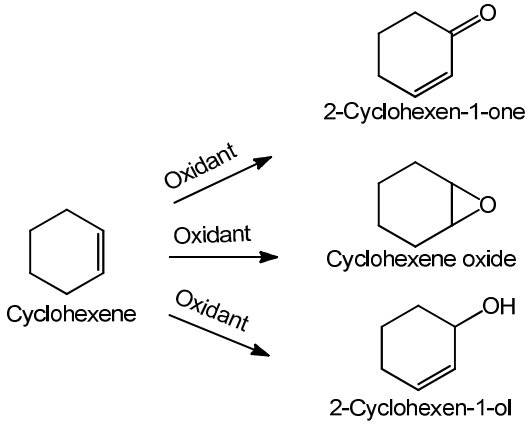

Fig. 1. The proposed reaction scheme for the selective oxidation of cyclohexene

2. Experimental

2.1 Materials synthesis

2.1.1 Au nanoparticle synthesis

Au nanoparticles were prepared by adapting the synthetic method described by Liu et al.[28] $HAuCl_4.3H_2O$ (24 mg) (Alfa Aesar, 99.99% purity) was dissolved in ethylene glycol (1 mL, Fisher Scientific >99%). To the solution, polyvinylpyrrolidone (22 mg, MW 40000, Alfa Aesar) was added followed by a further 6 mL of ethylene glycol and mixed for 10 minutes. Sodium borohydride (30 mg) was then added to the mixture and heated at 80 °C under N_2 for 30 minutes. The nanoparticles were isolated by the addition of acetone followed by centrifugation at 3500 rpm. In this way the nanoparticles were washed in acetone and then separated by centrifugation three times. The nanoparticles were then dispersed in deionised water. The method was found to produce Au nanoparticles of 2.5 ± 0.7 nm size, as shown in the supporting information (Figure S1).

2.1.2 Silica monolith synthesis

The monolith design was based upon existing designs and dimensions to ensure good thermal control. [11,29] Mesoporous silica monoliths were prepared by a modification of the method established by Fletcher et al.[11,29] Poly(ethylene oxide) (MW 200000, 0.122 g, Sigma Aldrich) was added to a solution of acetic acid (0.02 M, 1.6 mL, Aldrich, purity 97.9%) and stirred for 1 h (with a magnetic stirrer at 200 rpm) in an ice bath until fully homogeneous. Tetramethylorthosilicate (TMOS) (800 µl, Sigma Aldrich, purity 98%) was added to the solution over a period of 1 h until once again homogeneous. The solution was subsequently poured into a plastic mould (length 6 cm, internal diameter 0.45 cm), closed at both ends using poly(tetrafluoroethylene) (PTFE) thread seal tape. This was then aged at 40 °C for 3 days. The gel monolith was removed from the mould and washed thoroughly with deionised water to remove any trace residues. The monolith was then immersed in an incubator containing ammonia hydroxide solution (1 M). The solution was heated to ~82 °C for 24 h, to form a mesoporous network within the material. This was followed by further washing with deionised water to remove residual ammonium hydroxide until pH 7 was achieved. The monolith was dried at 40 °C for 1 day. The clean and dry monolith rods were heated at 600 °C for 3 h under air flow to remove the remaining poly(ethylene oxide). The rod was then cut to a 4 cm length, and linked to a borosilicate tube (Smith Scientific) *via* a PTFE heat shrinkable tube. This was heated in an oven at 350 °C for a 1 hr to seal the tube and encapsulate the monolithic rod.

2.1.3 Au nanoparticle impregnated silica monoliths synthesis

Au nanoparticle impregnated silica monoliths were prepared as described above, however after addition of the tetramethylorthosilicate, one hour after this was homogeneously mixed, the Au nanoparticle suspension in water was also added (0.4 M, 150 µl). The resulting mixture was then mixed until homogenous (0.5 h). The synthesis was then completed following the same process described above for the Au free monolith.

2.1.4 Au-thiol functionalized silica monolith

Once synthesised, a mesoporous silica monolith can be functionalized by incorporating a variety of useful functional groups such as: vinyl-, allyl-, amino-propyl and sulphur.[12,30] Functionalizing the silica monolith with these examples offer additional binding sites for ligands (vinyl-, allyl- and amino-propyl) that require a specific environment. In the present case thiolation of the monolith was performed to anchor Au nanoparticles. As the Au-S bond

is relatively strong and the thiolate ligand is also reasonably durable on the silica surface, the Au nanoparticles are stabilized.[31,32] Typically, functionalization takes place in two steps (i) functionalizing the surface of the monolith with thiol groups and (ii) anchoring Au nanoparticles to the sulfur containing functional groups. A 0.06 M solution of (3-mercaptopropyl)trimethoxysilane (MPTES) (Sigma Aldrich, purity 95%) in toluene (4 mL) was passed through the monolith at a flow rate of 40 µl min^{-1} at 100 °C in one direction, followed by a reverse flow from the opposite direction.[1] The monolith was then washed by passing toluene (4 mL), methanol (4 mL), and water (4 mL) at a flow rate of 40 µl min^{-1}. Finally, the Au nanoparticle suspension in water (3 mL, equivalent Au atom content 0.02 M) was passed through the functionalized monolith at a flow rate of 10 µl min^{-1} at room temperature. To ensure the removal of polyvinylpyrrolidone, the monolith was washed twice with water (3 mL) at a flow rate of 10 µl min^{-1}.

2.2 Characterization of catalysts

All samples were analysed via a JEOL 2010 Transmission Electron Microscopy (TEM) operated at 200 kV. Images were collected using a Gatan Ultrascan 4000 digital camera operated by Digital Micrograph software. Samples were dispersed in ethanol and deposited on 300-mesh carbon-coated copper grids and dried under ambient conditions. Au metal contents were determined by inductively coupled plasma optical emission spectroscopy (ICP-OES, Perkin Elmer Optical Emission Spectrometer Optima 5300 DV) after microwave digestion of the samples in 2 ml HNO_3 (Romil SPA grade 70%), 2 ml HCl (Romil SPA grade 60 %) at 200 °C (CEM-MARS microwave reactor) followed by aqueous dilution. Bulk compositions are ±10%. Scanning electron microscopy images were acquired via a Zeiss EVO 60 instrument and Oxford Instruments Inca System 350 under the pressure of 10^{-2} Pa and an electron acceleration voltage of 20 kV. Catalyst powder was adhered to double coated conductive carbon tape and attached to the specimen holder. BET surface areas and pore volumes were determined via N_2 physisorption using a Micrometrics TriStar porosimeter. Powder X-ray diffraction (PXRD) measurements were carried out using monochromated Cu K_α radiation (λ=0.1542 nm) on a PANalytical Empyrean series 2 diffractometer. Subsequent analysis of the diffractograms was performed in HighScore Plus (2013, PANalytical B.V.) with the ICDD's PDF-2 2012 database. X-ray photoelectron spectra were acquired on the UK National EPSRC XPS Users' Service (NEXUS) Kratos Axis Nova XP spectrometer with a monochromated Al K_α excitation source (1486.7 eV). Samples were mounted in powdered

form on carbon tape, pressed with a spatula, after pre-attaching the carbon tape to a stainless steel plate containing two holes, that act as wells into which to load the powder. A wide analysis area (300 × 700 μm) x-ray spot and charge compensation was used throughout all measurements. Energies are referenced to adventitious carbon at 284.4 eV. Spectral analysis was performed using CasaXPS.

2.3 Catalytic testing

A schematic of the reactor set up is depicted in Fig. 2. Controlled flow reactions were performed using acetonitrile (5 mL, Fisher, 99.96 % purity) as the solvent. The reactants 0.35 mmol cyclohexene (Sigma Aldrich 99.0 % purity) and 0.35 mmol of the oxidant in solution were mixed with the acetonitrile solvent at room temperature and were passed through the silica monolith at a constant flow rate of 12 μl min^{-1} using a Chemyx Fusion 100 Syringe Pump. The monolith microreactor was heated up to the required temperature (30 ^{o}C) and remained there for 1 hr. This ensured homogeneous temperature throughout the monolith structure during reaction. The reaction mixture travelled an 18 cm path length inside the furnace before reaching the monolith which ensured that the monolith and the passing liquid are at the same temperature thus minimising heat transfer limitations. This rate was chosen to ensure that before the reactants reached the monolith, they were able to equilibrate for 15mins.Two different oxidants were used in this study: hydrogen peroxide, (Sigma Aldrich, 30 wt.% in H_2O) and tert-butyl hydroperoxide (TBHP), (Sigma Aldrich, 5.0 – 6.0 M in decane). To maintain constant temperature the monolith was contained in a Model 7971 column heater (Jones Chromatography Ltd) held at 30 ± 0.1 $^{\circ}$C. The mixture eluted from the monolith was collected in a vial and analysed by gas chromatography, using a Bruker Scion 456-GC equipped with a flame ionisation detector and a Zebron ZB-5 (5%-phenyl-95%-dimethylpolysiloxane) capillary column. GC-MS was performed using an Agilent 6890 GC equipped with an Agilent 5973N. The detection limit for the analytical systems used equates to 0.2% conversion. Quadrupole mass spectrometer and an RXI-5MS (5%- phenyl-95 %-dimethylpolysiloxane) capillary column. Conversion and selectivities were calculated using equations S1 and S2, found in the supporting information.

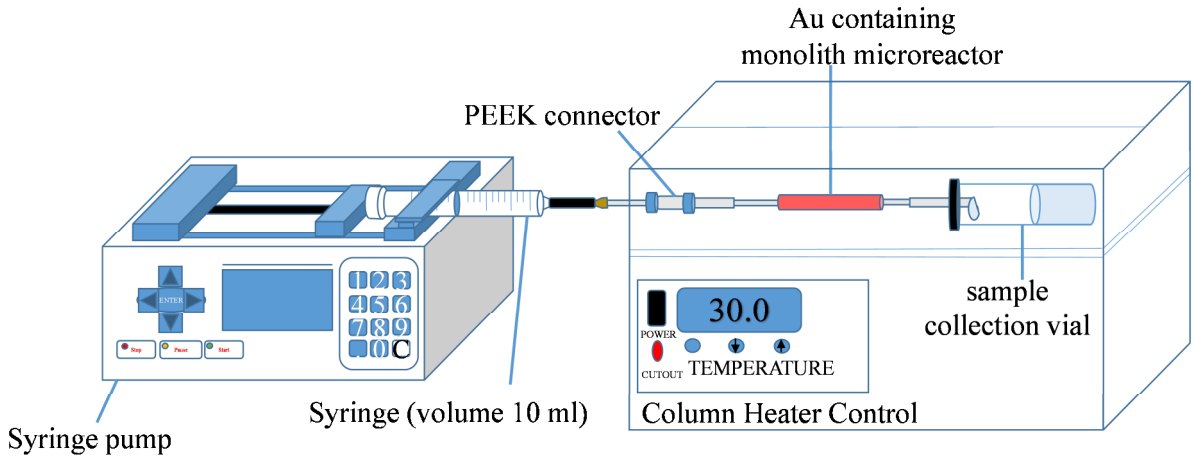

Fig. 2. Schematic of continuous flow system for silica monolith catalytic testing

3 Results and Discussion

3.1 SEM, TEM, ICP-OES, BET, PXRD and XPS

Silica monoliths in general may adapt a variety of structural morphologies depending on the synthesis procedure followed. These morphologies are governed primarily on the molecular weight of the starting polymer precursor as well as the ratio of water to silane. Alteration of the above parameters may lead to a variety of polymorphs, namely: (i) Air-in-silica, (ii) Silica-in-air and (iii) Bicontinuous.[29] In this work the "sponge like" bicontinuous monolithic structure reported by Fletcher et al.[29] was targeted as it maximises the available surface area and pore volume. The bicontinuous "sponge like" monolith structure can be obtained under specific reaction conditions and is characterized by a "continuous mutually conjugated domains and hyperbolic interfaces".[33] SEM images in Fig. 3 show that this was successfully achieved by following the synthetic protocol described above, which can be seen to lead to a "coral like" structure seen in the Au-free monolith in Fig. 3a.[34] The image is typical of the bicontinuous monolithic morphology.[29,35–37] The SEM measurements suggest that the coral like network is preserved when Au is incorporated in the monolith by either method (Fig. 3b and 3c). The Au nanoparticles, highlighted by red circles in Fig. 3b and 3c, appear as bright spots within the SiO_2 network. Critically, the particles observed in Fig. 3b appear much larger than those in Fig. 3c which suggests heavy agglomeration of Au in the case of the Au impregnated monolith.

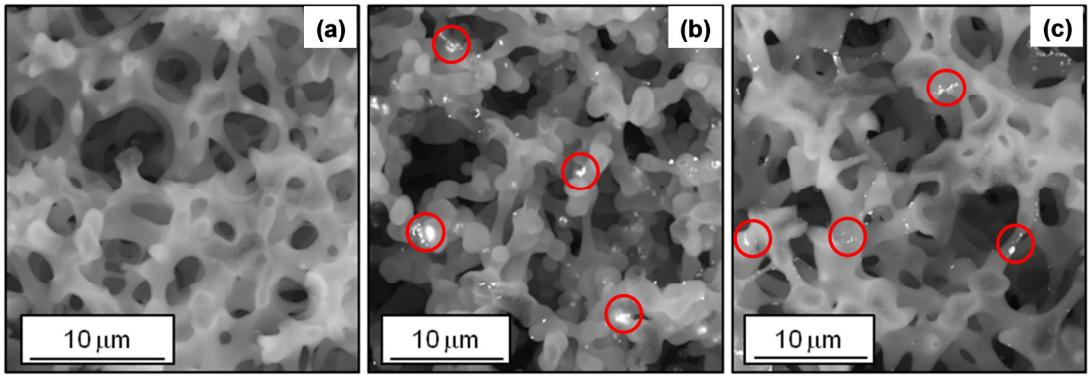

Fig. 3. SEM image of (a) Au free monolith, (b) Au impregnated monolith and (c) Au-thiol functionalized monolith.

Although, the incorporation of Au does not change the shape of the host SiO_2 pore network, the BET measurements (Table 1) suggest that the Au doped monoliths have lower surface area and pore volume while the overall pore size is increased. This is understood in terms of restricted diffusion of N_2 molecules in the micropores of the monolith due to blocking with Au nanoparticles during the N_2 physisorption measurement.[38–40] Blocking of the small pores of the mesostructure with Au particles or particle aggregates leads to a lower overall monolith surface area. On the other hand blocking of the small pores will increase the average pore size of the monolith as diffusion of particles takes place only at the larger unblocked pores. Interestingly this effect appears to be more pronounced in the case of the thiol functionalized Au monolith as compared to the impregnated one. This suggests that a larger number of Au nanoparticles must be present, which amplifies the blocking effect. To further elucidate this point TEM and ICP-OES measurements were performed.

Table 1. Surface area and porosity measurements of the various monoliths

Sample	BET surface area / $m^2 g^{-1}$	Pore volume / $cm^3 g^{-1}$	Pore size / nm
Au / thiol monolith	160	0.6	16.2
Au impregnated monolith	191	0.7	15.4
Au - free monolith	210	0.9	11.6

Fig. 4 shows the elemental (ICP-OES) analysis for the two Au based monoliths. The analysis was performed by dissecting the monolith rod into 4 sections of 1 cm length. From each section, a piece of ~0.1 cm was cut and digested following the method described in the

experimental section. The key point to note is that in both cases the Au content appears to be nearly homogeneous across the length of each monolith, as was desired. The final weight % loading determined by ICP-OES is similar in both cases: the impregnated monolith had a Au content of 2.7 wt% ± 0.2% across the monolith rod, while for the thiol functionalized monolith there was a Au content of 1.2 wt% ± 0.3%. This similarity in Au content (around a factor of two) confirms that the very significant differences in agglomeration are unlikely to be due merely to different Au loadings. It should also be noted that there is a small loss of Au from the nominal loading of 4.7 wt% in the case of the impregnated method (likely due to washing steps removing any free material during the synthesis), but for the thiol functionalized monolith a saturation (based on the number of thiol groups) is reached despite washing through a large excess of Au nanoparticles (which if all incorporated would yield a 9.4% nominal loading). In the latter case it should be noted that to minimize waste of valuable Au the nanoparticles not tethered within one monolith could be collected after pumping through the first monolith and used directly to load further monoliths with Au nanoparticles.

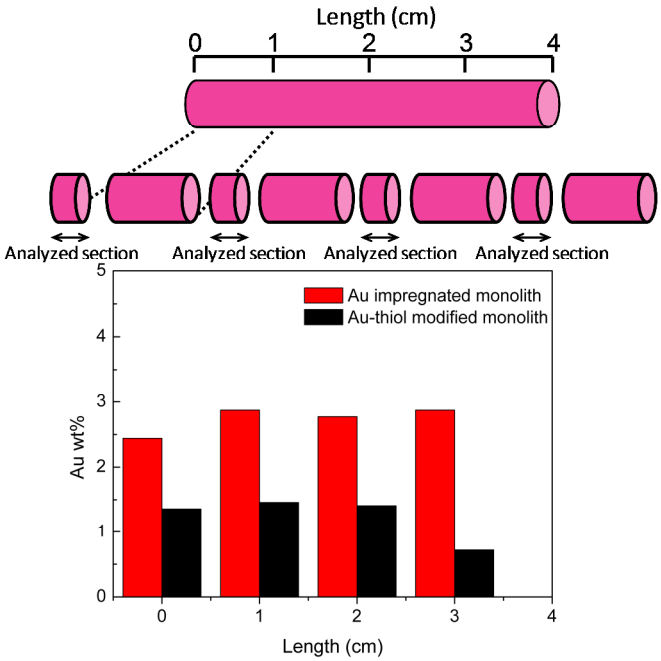

Fig. 4. ICP-OES results taken at 1 cm cross sections of the two monoliths.

Fig. 5 shows representative TEM images and the particle size histograms for the two Au monoliths. It can be seen that the Au nanoparticles of the thiol functionalized Au monolith have a relatively narrow particle size distribution (average size of 6.8 ± 1.4 nm). Impregnation of the monolith with Au nanoparticles led to a vastly broader particle size

distribution (average size 49.5 ± 26.5 nm diameter) with a maximum size of 110 nm, due to severe agglomeration. The difference in Au particle size between the two monoliths is attributed to the heat treatment. The monolith synthetic protocol requires calcination at 600 °C to produce the final material. In the case of the impregnated monolith the Au nanoparticles are present in the monolith when the calcination process takes place leading to strong agglomeration of the particles. In the case of the thiol functionalized monolith the Au nanoparticles are added to the monolith after the calcination step, thus they are protected from agglomeration which leads to led to a more uniform particle size distribution.[41]

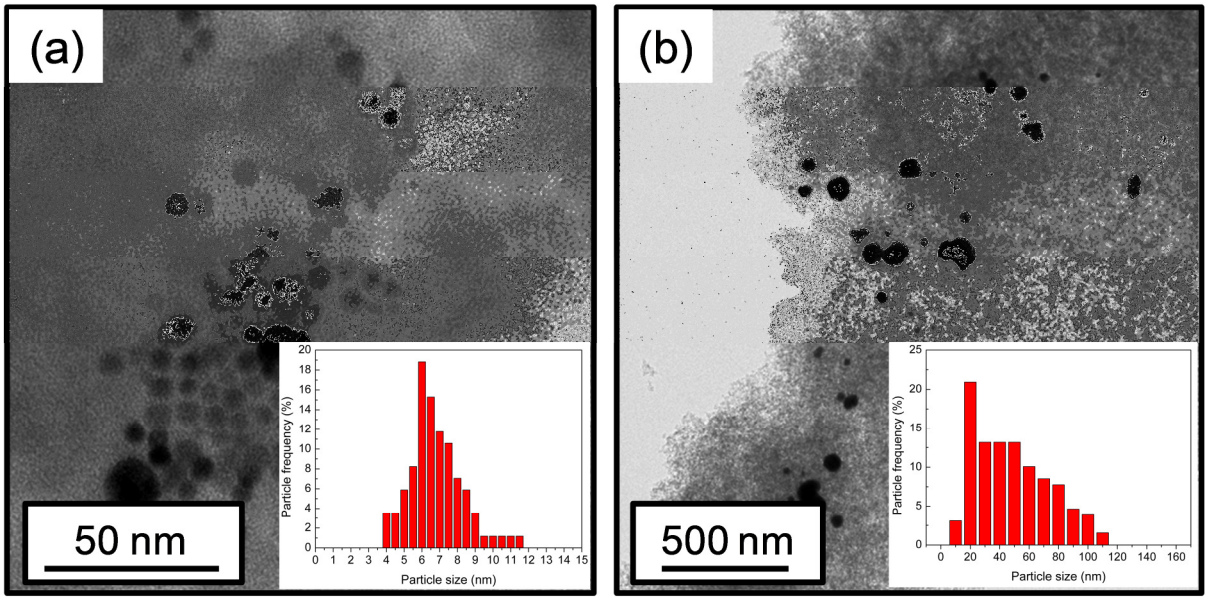

Fig. 5. TEM and particle size distribution diagrams of: (a) Au thiol-functionalized monolith and (b) Au impregnated monolith.

Further confirmation of the general trend in particle size difference between the two monoliths was obtained via PXRD measurements. Fig. 6a shows that the Au particles present in both samples possess the same four crystal planes with the {111} plane being the most dominant in both cases. The broadening of the peaks in the case of the thiol modified Au monolith suggests that the Au particle size is smaller than that of the impregnated monolith.[9] By utilising Scherrer's equation, an average crystallite size was obtained (Table 2). As can be seen, the trend in particle sizes for the Au-thiol monolith is concordant between the PXRD and TEM. It is worth noting that the TEM particle size is a number average (counted once per particle), whereas PXRD is an electron weighted average; PXRD therefore is relatively biased towards large particles [42] in the case of the thiol modified small particles this likely accounts for the numerical difference between the two methods. For the

impregnated sample the large range of particle sizes and possibility many particles are present as agglomerates also may lead to an apparent numerical inconsistency, but this time due to the difference between apparent particle size inferred from contrast in bright field TEM images vs. PXRD which measures crystallite rather than particle size. The key point however is both techniques indicate the general result that the thiol modified monolith method affords much improved size control and thus leads to smaller particles. Clearly, despite the relatively higher Au content of the impregnated monolith, the available Au surface area is relatively lower as compared to the thiol functionalized monolith due to the severe agglomeration of the Au nanoparticles. This effect is also seen very dramatically in the XPS spectra shown in Fig. 6b which show, after correction to the Si 2p substrate signal, that the XPS visible Au is 8 times greater for the thiol modified sample as compared to the impregnated one, despite the slightly lower bulk gold content of the former. This confirms the loss of surface Au (and consequent loss of catalytic sites) as a result of Au agglomeration in the impregnated catalyst, since the Au signal will largely originate from near the surface of the nanoparticles and so gold buried deep with the larger agglomerated particles will not be seen (emitted electrons have a kinetic energy of 1403 eV, corresponding to a typical mean free path escape depth of 1.8 nm).[43] Additionally, Fig. 5c shows the S 2p XP spectra which clearly demonstrate the successful functionalization of the monolith with the thiol groups.

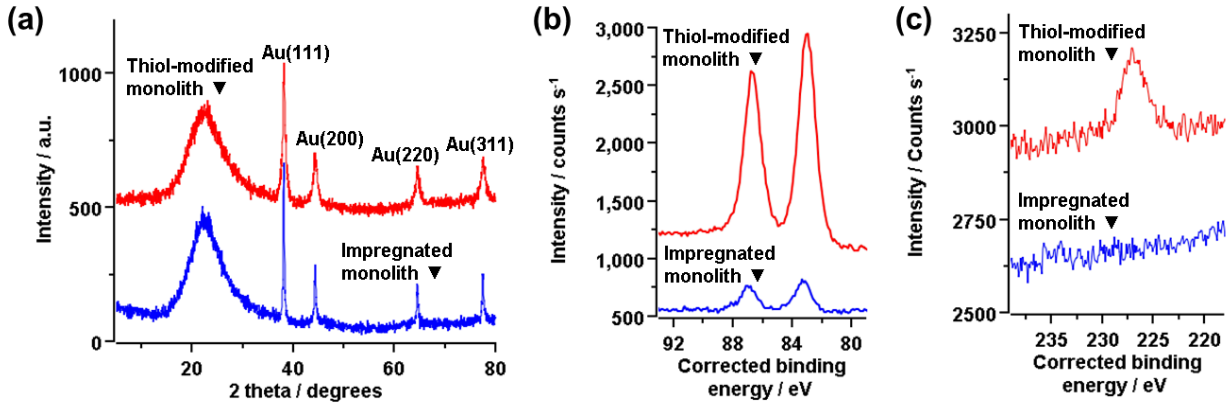

Fig. 6. For gold catalyst monoliths impregnated (bottom) and thiol-modified (top): (a) PXRD data, specific dominant crystallographic planes are indicated on the figure; (b) Au 4f region XP spectra; and, (c) S 2s region XP spectra. In each case (a-c) data for two samples are offset for clarity. XPS binding energy scale corrected to C 1s at 284.4 eV.

Table 2. Au particle size distribution via TEM and PXRD.

Catalyst	TEM average particle size (nm)	PXRD average crystallite size (nm)
Au - Impregnated monolith	49.5 ± 26.5	22.0 ± 10.0
Au - thiol modified monolith	6.8 ± 1.4	11.0 ± 5.0

3.2 Catalytic testing

The Au free and the two Au containing monoliths were tested for the selective oxidation of cyclohexene using acetonitrile as the solvent at the very mild temperature of 30 °C. The reaction was studied using two different oxidants: tert-butyl hydroperoxide (TBHP) and hydrogen peroxide (H_2O_2).[22] The molar ratio of reagent to oxidant was kept to 1:1. The results are summarised in Table 3. The pure silica monolith was found to be inactive for the selective oxidation of cyclohexene at 30 °C with both TBHP and H_2O_2. The impregnated monolith was found to lead to low conversion of cyclohexene (≤ 3 % conversion) using both oxidants. This is attributed to the relatively low surface area of the heavily agglomerated Au nanoparticles present in this monolith. Under these low conversions, the selectivity of the reaction was found to be different when the two oxidants were used with H_2O_2 favouring cyclohexene oxide (58.4 % selectivity) while TBHP favouring the formation of 2-cyclohexen-1-ol (51.5 % selectivity).

Table 3. Cyclohexene oxidation on Au impregnated and Au free monoliths using tert-butyl hydroperoxide (TBHP) and hydrogen peroxide (H_2O_2) as the oxidants at 30 °C. Details of the calculation of conversion and TOF are given in the ESI. The conversion is normalised to account for material still trapped within the monolith at the end of the reaction.

Catalyst	Oxidant	Conversion / %	TOF	Cyclohexene oxide S / %	2-Cyclohexen-1-one S / %	2-Cyclohexen-1-ol S / %
Au free Monolith	TBHP	< 0.2	n/a	0	0	0
Au/Monolith (impregnated)	TBHP	3.1	184	30.2	18.3	51.5
Au/Monolith (thiol modified)	TBHP	18.3	342	2.5	81.5	16.0
Au free Monolith	H_2O_2	< 0.2	n/a	0	0	0
Au/Monolith (impregnated)	H_2O_2	2.8	167	8.4	18.5	23.1
Au/Monolith (thiol modified)	H_2O_2	2.7	51	56.7	22.7	20.6

S - % selectivity

TOF – Turnover frequency (cyclohexene molecules per surface Au atom, per hour)

As might be expected owing to the higher surface area, the thiol functionalized monolith was found to be relatively more reactive than the impregnated monolith with the conversion reaching 18.3% when TBHP was used as the oxidant. This also confirms that there is no strongly deleterious poisoning effect resulting from the presence of a small number of sulfur binding sites present in the material. Normalization to the metal surface area in the form of turnover frequencies (TOFs), also given in Table 3, gives additional insight into the mechanism by which the mass activity enhancement observed may be occurring. TOF values are in the high end of the range expected for room temperature cyclohexene oxidation using

peroxide oxidants; speculatively this is perhaps due to less mass transfer limitations in a flow reactor, rather than the batch systems commonly reported.[44] However, it is interesting to note that TOF values are relatively comparable for either oxidant in the case of the impregnated monolith, but differ somewhat between the two oxidants in the case of the thiol modified monolith. As can be seen the thiol modified TOF values fall either side of the impregnated TOF values (suggesting in general terms much of the mass activity enhancement seen is likely due to higher surface area). We speculate the difference in the case of the thiol modified monolith with different oxidants may be due to the presence of the thiol anchoring agent which induces an increased hydrophobicity in the silica monolith [45,46] limiting the access of H_2O_2, thus lowering the rate of reaction. The slight increase of TOF (factor of 2) when using organic TBHP as oxidant with the thiol modified monolith compared to the impregnated monolith could either be due again to the hydrophobicity, or due to better access of reactants within the monolith structure – large Au agglomerates can be expected to potentially cause more blockages in the pore structure. Both these factors can be seen as potentially contributory to the mechanism by which our method of dispersing small gold nanoparticles within the monolith structure leads to a substantial improvement in mass activity for practical chemical processing. The results suggest that tailoring the selectivity of the selective oxidation reaction is driven by both the oxidizing agent and the method used to functionalize the monolith with Au nanoparticles. Furthermore, the XPS data of both monolith catalysts (Fig. 6b) are indicative of Au in the metallic state with very limited variation in the peak centres – Au $4f_{7/2}$ 283.1 and 283.3 eV for the modified and unmodified catalysts respectively; shifts for oxidation to Au(I) are typically 1 eV or more.[47] XPS therefore excludes the possibility the improved catalysis observed is due to changes in the electronic structure rather than simply as a result of the dramatically improved particle size control when using the thiol modified monolith.

Conclusions

In summary, we have shown how two simple methods can be used to prepare mesoporous monolithic reactors functionalized evenly along their length with Au nanoparticles. These methods consist of (i) impregnation of Au nanoparticles in the porous network during monolith synthesis, (ii) functionalizing the monolith with sulfur groups and then passing Au along the monolith, forming Au-thiol bonds. While both methods successfully achieved even distribution of gold nanoparticles along the length of the monolithic microreactor, the two

methods were found to lead to very different Au particle sizes and therefore available catalytic Au surface area, as seen by the XPS and TEM. It was found that a pure silica monolith was inactive for the oxidation reaction. The incorporation of Au proved essential in utilising the monoliths for continuous flow selective oxidation catalytic microreactors. The Au free monoliths were found to be unreactive at 30 $^{\circ}$C. The thiol functionalized was found to be more active when using TBHP as oxidant as compared to the impregnated monolith due to the better dispersity and higher surface area of Au and in spite of the presence of sulfur. Additionally, the oxidation reaction on the Au-thiol functionalized monolith was found to depend on the type of oxidant used with tert-butyl hydroperoxide being more active than H_2O_2, likely due to the thiol induced hydrophobicity of the monolith. Overall the results point to the use of post synthetic surface modification to anchor nanoparticles as a highly effective strategy for evenly incorporating catalytically active nanoparticles within monolithic flow reactors.

Acknowledgements

GK acknowledges the Royal Society for funding. MJT acknowledges the award of a PhD scholarship from Hull University. MTA acknowledges funding from the Saudi Arabian Ministry of Education. SKB gratefully acknowledges fellowship support from both the Durham University Addison Wheeler scheme and the Leverhulme Trust's Early Career Fellowship scheme. X-ray photoelectron spectra were obtained at the National EPSRC XPS Users' Service (NEXUS) at Newcastle University, an EPSRC Mid-Range Facility.

References

[1] C. Della Pina, E. Falletta, M. Rossi, Update on selective oxidation using gold, Chem. Soc. Rev. 41 (2012) 350. doi:10.1039/c1cs15089h.

[2] A.D. Jewell, E.C.H. Sykes, G. Kyriakou, Molecular-scale surface chemistry of a common metal nanoparticle capping agent: Triphenylphosphine on Au(111), ACS Nano. 6 (2012) 3545–3552. doi:10.1021/nn300582g.

[3] M. Haruta, T. Kobayashi, H. Sano, N. Yamada, Novel gold catalysts for the oxidation of carbon monoxide at a temperature far below 0.DEG.C., Chem. Lett. (1987) 405–408. doi:10.1246/cl.1987.405.

[4] M. Turner, V.B. Golovko, O.P.H. Vaughan, P. Abdulkin, A. Berenguer-Murcia, M.S. Tikhov, et al., Selective oxidation with dioxygen by gold nanoparticle catalysts derived from 55-atom clusters., Nature. 454 (2008) 981–983. doi:10.1038/nature07194.

[5] P. Landon, J. Ferguson, B.E. Solsona, T. Garcia, A.F. Carley, A.A. Herzing, et al., Selective oxidation of CO in the presence of H2, H2O and CO2 via gold for use in fuel cells., Chem. Commun. (Camb). (2005) 3385–3387. doi:10.1039/b505295p.

[6] G. Kyriakou, S.K. Beaumont, S.M. Humphrey, C. Antonetti, R.M. Lambert, Sonogashira Coupling Catalyzed by Gold Nanoparticles: Does Homogeneous or Heterogeneous Catalysis Dominate?, ChemCatChem. 2 (2010) 1444–1449. doi:10.1002/cctc.201000154.

[7] S.K. Beaumont, G. Kyriakou, R.M. Lambert, Identity of the active site in gold nanoparticle-catalyzed Sonogashira coupling of phenylacetylene and iodobenzene., J. Am. Chem. Soc. 132 (2010) 12246–8. doi:10.1021/ja1063179.

[8] A. Corma, P. Serna, Chemoselective Hydrogenation of Nitro Compounds with Supported Gold Catalysts, Science (80-.). (2006) 332–334.

[9] R. Munirathinam, J. Huskens, W. Verboom, Supported Catalysis in Continuous-Flow Microreactors, Adv. Synth. Catal. 357 (2015) 1093–1123. doi:10.1002/adsc.201401081.

[10] A. Sachse, A. Galarneau, B. Coq, F. Fajula, Monolithic flow microreactors improve fine chemicals synthesis, New J. Chem. 35 (2011) 259. doi:10.1039/c0nj00965b.

[11] P. He, S.J. Haswell, P.D.I. Fletcher, S.M. Kelly, A. Mansfield, Scaling up of continuous-flow, microwave-assisted, organic reactions by varying the size of Pd-functionalized catalytic monoliths, Beilstein J. Org. Chem. 7 (2011) 1150–1157. doi:10.3762/bjoc.7.133.

[12] J. Ou, Z. Liu, H. Wang, H. Lin, J. Dong, H. Zou, Recent development of hybrid organic-silica monolithic columns in CEC and capillary LC, Electrophoresis. 36 (2015) 62–75. doi:10.1002/elps.201400316.

[13] C. Park, Y. La, T.H. An, H.Y. Jeong, S. Kang, S.H. Joo, et al., Mesoporous monoliths of inverse bicontinuous cubic phases of block copolymer bilayers, Nat. Commun. 6 (2015) 6392. doi:10.1038/ncomms7392.

[14] A. El Kadib, R. Chimenton, A. Sachse, F. Fajula, A. Galarneau, B. Coq, Functionalized inorganic monolithic microreactors for high productivity in fine chemicals catalytic synthesis, Angew. Chemie - Int. Ed. 48 (2009) 4969–4972. doi:10.1002/anie.200805580.

[15] S. Tang, Y. Guo, C. Xiong, S. Liu, X. Liu, S. Jiang, Nanoparticle-based monoliths for chromatographic separations., Analyst. 139 (2014) 4103–17. doi:10.1039/c4an00593g.

[16] J. Randon, S. Huguet, C. Demesmay, A. Berthod, Zirconia based monoliths used in hydrophilic-interaction chromatography for original selectivity of xanthines, J. Chromatogr. A. 1217 (2010) 1496–1500. doi:10.1016/j.chroma.2009.12.077.

[17] W. Sun, Q. Li, S. Gao, J.K. Shang, Exceptional arsenic adsorption performance of hydrous cerium oxide nanoparticles: Part B. Integration with silica monoliths and

dynamic treatment, Chem. Eng. J. 185-186 (2012) 136–143. doi:10.1016/j.cej.2012.01.060.

[18] G. Wang, D. Kundu, H. Uyama, One-pot fabrication of palladium nanoparticles captured in mesoporous polymeric monoliths and their catalytic application in C–C coupling reactions, J. Colloid Interface Sci. 451 (2015) 184–188. doi:10.1016/j.jcis.2015.03.061.

[19] R. Poupart, B. Le Droumaguet, M. Guerrouache, B. Carbonnier, Copper nanoparticles supported on permeable monolith with carboxylic acid surface functionality: Stability and catalytic properties under reductive conditions, Mater. Chem. Phys. 163 (2015) 446–452. doi:10.1016/j.matchemphys.2015.07.064.

[20] I. Miguel-García, M. Navlani-García, J. García-Aguilar, Á. Berenguer-Murcia, D. Lozano-Castelló, D. Cazorla-Amorós, Capillary microreactors based on hierarchical SiO2 monoliths incorporating noble metal nanoparticles for the Preferential Oxidation of CO, Chem. Eng. J. 275 (2015) 71–78. doi:10.1016/j.cej.2015.04.020.

[21] L. Wang, H. Wang, P. Hapala, L. Zhu, L. Ren, X. Meng, et al., Superior catalytic properties in aerobic oxidation of olefins over Au nanoparticles on pyrrolidone-modified SBA-15, J. Catal. 281 (2011) 30–39. doi:10.1016/j.jcat.2011.03.029.

[22] E.L. Pires, J.C. Magalhães, U. Schuchardt, Effects of oxidant and solvent on the liquid-phase cyclohexane oxidation catalyzed by Ce-exchanged zeolite Y, Appl. Catal. A Gen. 203 (2000) 231–237. doi:10.1016/S0926-860X(00)00496-8.

[23] K.K. Zhu, J.C. Hu, R. Richards, Aerobic oxidation of cyclohexane by gold nanoparticles immobilized upon mesoporous silica, Catal. Letters. 100 (2005) 195–199. doi:10.1007/s10562-004-3454-5.

[24] P. Wu, Z. Xiong, K.P. Loh, X.S. Zhao, Selective oxidation of cyclohexane over gold nanoparticles supported on mesoporous silica prepared in the presence of thioether functionality, Catal. Sci. Technol. 1 (2011) 285. doi:10.1039/c0cy00025f.

[25] M.D. Hughes, Y.-J. Xu, P. Jenkins, P. McMorn, P. Landon, D.I. Enache, et al., Tunable gold catalysts for selective hydrocarbon oxidation under mild conditions., Nature. 437 (2005) 1132–1135. doi:10.1038/nature04190.

[26] A. Corma, P. Esteve, A. Martnez, Solvent Effects during the Oxidation of Olefins and Alcohols with Hydrogen Peroxide on Ti-Beta Catalyst: The Influence of the Hydrophilicity-Hydrophobicity of the Zeolite, J. Catal. 161 (1996) 9. doi:10.1006/jcat.1996.0157.

[27] N. Yu, Y. Ding, A.Y. Lo, S.J. Huang, P.H. Wu, C. Liu, et al., Gold nanoparticles supported on periodic mesoporous organosilicas for epoxidation of olefins: Effects of pore architecture and surface modification method of the supports, Microporous Mesoporous Mater. 143 (2011) 426–434. doi:10.1016/j.micromeso.2011.03.030.

[28] J. Liu, S. Zou, S. Li, X. Liao, Y. Hong, L. Xiao, et al., A general synthesis of mesoporous metal oxides with well-dispersed metal nanoparticles via a versatile sol–gel process, J. Mater. Chem. A. 1 (2013) 4038. doi:10.1039/c3ta00570d.

[29] P.D.I. Fletcher, S.J. Haswell, P. He, S.M. Kelly, A. Mansfield, Permeability of silica monoliths containing micro- and nano-pores, J. Porous Mater. 18 (2011) 501–508. doi:10.1007/s10934-010-9403-3.

[30] R. Göbel, P. Hesemann, A. Friedrich, R. Rothe, H. Schlaad, A. Taubert, Modular Thiol-Ene Chemistry Approach towards Mesoporous Silica Monoliths with Organically Modified Pore Walls, Chem. - A Eur. J. 20 (2014) 17579–17589. doi:10.1002/chem.201403982.

[31] J.C. Love, L.A. Estroff, J.K. Kriebel, R.G. Nuzzo, G.M. Whitesides, Self-assembled monolayers of thiolates on metals as a form of nanotechnology, 2005. doi:10.1021/cr0300789.

[32] E. Skrzyńska, J. Ftouni, A.S. Mamede, A. Addad, M. Trentesaux, J.S. Girardon, et al., Glycerol oxidation over gold supported catalysts - "two faces" of sulphur based anchoring agent, J. Mol. Catal. A Chem. 382 (2014) 71–78. doi:10.1016/j.molcata.2013.11.007.

[33] B. Gaweł, K. Gaweł, G. Øye, Sol-gel synthesis of non-silica monolithic materials, Materials (Basel). 3 (2010) 2815–2833. doi:10.3390/ma3042815.

[34] S. Altmaier, K. Cabrera, Structure and performance of silica-based monolithic HPLC columns, J. Sep. Sci. 31 (2008) 2551–2559. doi:10.1002/jssc.200800213.

[35] J. Le Bideau, M.Y. Miah, A. Vioux, F. Fajula, A. Galarneau, Bimodal porous silica monoliths obtained by phase separation in non-aqueous media, J. Mater. Chem. 20 (2010) 964. doi:10.1039/b918412k.

[36] A. Ghanem, T. Ikegami, Recent advances in silica-based monoliths: Preparations, characterizations and applications, J. Sep. Sci. 34 (2011) 1945–1957. doi:10.1002/jssc.201100086.

[37] D. Zhao, J. Sun, Q. Li, G.D. Stucky, S. Barbara, Morphological Control of Highly Ordered Mesoporous Silica SBA-15 Mesoporous materials are of great interest to the materials community because their pore structures as well as catalytic , adsorbed , conductive and magnetic ordered large mesoporous silica , Communications. (2000) 275–279.

[38] W. Chen, J. Zhang, Y. Di, Z. Wang, Q. Fang, W. Cai, Size controlled Ag nanoparticles within pores of monolithic mesoporous silica by ultrasonic irradiation, Appl. Surf. Sci. 211 (2003) 280–284. doi:10.1016/S0169-4332(03)00244-7.

[39] W. Chen, J. Zhang, L. Shi, Y. Di, Q. Fang, W. Cai, Characterization of sonochemically prepared silver-silica monolithic mesoporous nanocomposite, Compos. Sci. Technol. 63 (2003) 1209–1212. doi:10.1016/S0266-3538(03)00026-5.

[40] C. Huo, J. Ouyang, H. Yang, CuO nanoparticles encapsulated inside Al-MCM-41 mesoporous materials via direct synthetic route., Sci. Rep. 4 (2014) 3682. doi:10.1038/srep03682.

[41] G.M. Veith, A.R. Lupini, S. Rashkeev, S.J. Pennycook, D.R. Mullins, V. Schwartz, et al., Thermal stability and catalytic activity of gold nanoparticles supported on silica, J. Catal. 262 (2009) 92–101. doi:10.1016/j.jcat.2008.12.005.

[42] G.A. Somorjai, S.K. Beaumont, Conquering Catalyst Complexity: Nanoparticle Synthesis and Instrument Development for Molecular and Atomistic Characterisation Under In Situ Conditions, Top. Catal. 58 (2015) 560–572. doi:10.1007/s11244-015-0398-5.

[43] C.J. Powell, A. Jablonski, NIST Electron Inelastic-Mean-Free-Path Database, 2010.

[44] P. Bujak, P. Bartczak, J. Polanski, Highly efficient room-temperature oxidation of cyclohexene and d-glucose over nanogold Au/SiO2 in water, J. Catal. 295 (2012) 15–21. doi:10.1016/j.jcat.2012.06.023.

[45] A. Venkateswara Rao, R.R. Kalesh, Comparative studies of the physical and hydrophobic properties of TEOS based silica aerogels using different co-precursors, Sci. Technol. Adv. Mater. 4 (2003) 509–515. doi:10.1016/j.stam.2003.12.010.

[46] C. Xie, J. Hu, H. Xiao, X. Su, J. Dong, R. Tian, et al., Preparation of monolithic silica column with strong cation-exchange stationary phase for capillary electrochromatography, J. Sep. Sci. 28 (2005) 751–756. doi:10.1002/jssc.200400101.

[47] M.P. Casaletto, A. Longo, A. Martorana, A. Prestianni, A.M. Venezia, XPS study of supported gold catalysts: the role of Au0 and Au+d species as active sites, Surf. Interface Anal. 38 (2006) 1578–1587. doi:10.1002/sia.